American Mineralogist, Volume 64, pages 563–572, 1979

Agrellite, $Na(Ca,RE)_2Si_4O_{10}F$: a layer structure with silicate tubes

SUBRATA GHOSE AND CHE'NG WAN

Department of Geological Sciences, University of Washington
Seattle, Washington 98195

Abstract

Agrellite, $Na(Ca,RE)_2Si_4O_{10}F$, from the regionally metamorphosed agpaitic peralkaline rocks in Villedieu Township, Québec, is triclinic, space group $P\bar{1}$, with cell dimensions: a = 7.759(2), b = 18.946(3), c = 6.986(1)A, α = 89.88(2), β = 116.65(2), γ = 94.32(2)°; Z = 4. The crystal structure was determined by the symbolic addition method and refined by the method of least squares to an R factor of 0.045, based on 5343 reflections measured on an automatic single-crystal diffractometer. The average standard deviations in Na–O, Ca–O, and Si–O bond lengths are 0.004, 0.003, and 0.003A respectively.

Due to the presence of pseudo-C-center, the sodium polyhedra and the silicate tetrahedra occur in pairs, whose configurations are nearly identical. The crystal structure of agrellite consists of two different NaO_8 polyhedra which are distorted cubes, two each of CaO_5F octahedra and CaO_6F_2 polyhedra, and two different $[Si_8O_{20}]$ double chains. These double chains are hollow tubes, formed by the polymerization of two vlasovite-type $[Si_4O_{11}]$ single chains, consisting of corner-sharing four-membered rings. The silicate tubes, whose diameter is defined by a basket-shaped six-membered ring, run parallel to the c axis and are hexagonally close-packed in the (001) plane. The sodium atoms occurring in cavities cross-link these tubes to form sodium silicate layers parallel to the (010) plane; these layers alternate with the calcium polyhedral layers along the b axis to form a three-dimensional framework. The average Si–O bond length is 1.619A; the non-bridging Si–O bond lengths (av. 1.579A) are significantly shorter than the bridging ones (av. 1.632A). The average Na–O bond length within the NaO_8 polyhedra is 2.667A. Within the CaO_5F octahedra and CaO_6F_2 polyhedra the average Ca–O bond lengths are 2.374 and 2.595A, and the average Ca–F bond lengths are 2.197 and 2.430A, respectively. Along with narsarsukite, fenaksite, litidionite, canasite, and miserite, agrellite belongs to a distinct class of silicates, whose structures consist of silicate tubes.

Introduction

Agrellite is a recently described rock-forming silicate with the chemical composition: $(Na_{4.06}K_{0.07})(Ca_{7.30}RE_{0.47})(Mn,Fe,Sr,Ba,Mg,Sr)_{0.14}(Si_{15.61}Al_{0.03})O_{39.70}(F_{3.73}OH_{0.71})$. It is found in agpaitic peralkaline rocks of the Kipawa Complex, Villedieu Township, Témiscaming County, Québec, Canada (Gittins *et al.*, 1976). It occurs as prismatic white triclinic crystals (up to 10 cm long) in pegmatitic lenses and gneisses composed principally of albite, microcline, aegirine-augite, alkali amphibole, with or without eudialyte and nepheline, and sometimes hiortdahlite and other members of the wöhlerite group, mosandrite, britholite, miserite, vlasovite, calcite, fluorite, clinohumite, norbergite, zircon, biotite, phlogopite, galena, and an unnamed mineral (Ca $ZrSi_2O_7$). Gittins *et al.* (1976) have determined the chemical composition and crystallographic and optical properties of agrellite. For the purposes of the crystal-structure determination, the chemical composition of agrellite has been simplified to $Na(Ca_{1.905}RE_{0.095})Si_4O_{10}F$. The crystal structure of agrellite has been briefly reported by Ghose and Wan (1978a).

Crystal data

A small cleavage fragment of agrellite was ground to a sphere with a diameter of 0.25 mm (Bond, 1951), which was mounted on the computer-controlled single-crystal X-ray diffractometer (Syntex $P\bar{1}$). The unit-cell dimensions were determined by least-squares refinement of the 2θ values (between 30 and 40°) measured from 15 reflections, using mono-

0003–004X/79/0506–0563$02.00

chromatic Mo$K\alpha$ radiation (Table 1). The dimensions of the triclinic unit cell are in good agreement with those determined by Gittins *et al.* (1976), except that we have chosen the angle α as acute rather than obtuse, to maintain a right-handed axial system. An $N(z)$ test of the measured intensities indicated the centric space group $P\bar{1}$, which was subsequently confirmed by the crystal-structure determination.

Collection of the intensity data

The X-ray intensity data were collected from the single-crystal sphere on the Syntex $P\bar{1}$ diffractometer by the θ–2θ method, using Mo$K\alpha$ radiation monochromatized by reflection from a graphite "single" crystal and a scintillation counter. The variable-scan method was used, the minimum scan rate being 2°/min (50 kV, 12 mA). All reflections within $2\theta = 60°$ were measured, a total of 5343 reflections, out of which 1436 were below $3\sigma(I)$, where $\sigma(I)$ is the standard deviation of the intensity I, as determined from the counting statistics. For all reflections less than $0.7\sigma(I)$, the intensity was set to $0.7\sigma(I)$, regardless of whether the measured intensity was positive or negative. The measured intensities were corrected for Lorentz, polarization, and absorption factors.

Determination and refinement of the structure

The crystal structure has been determined by the symbolic addition method (Karle and Karle, 1966), using the computer program MULTAN (Germain *et al.*, 1971). 351 reflections with E values >1.8 were used for the phase determination. The phases of the following three reflections were chosen to define the origin:

h	k	l	E	Phase angle
1	−13	0	2.98	0°
4	−19	2	2.88	0°
4	0	−5	2.74	0°

In addition, the phase of the reflection $40\bar{8}$ (E = 2.58) was found to be 0°, using the Σ_2 relationship. The phases of the following five reflections were represented by symbols:

h	k	l	E	Final phase angle
2	0	−4	4.01	0°
4	12	−4	3.21	180°
8	9	0	2.55	0°
6	−6	0	2.37	180°
7	4	−4	2.34	0°

Table 1. Agrellite: crystal data

Agrellite, $Na(Ca,R.E.)_2Si_4O_{10}F$

Villedieu Township, Témiscaming County, Québec, Canada

Colorless transparent prisms, N.M.N.H. # 134022

Triclinic, $\bar{1}$

a(Å): 7.759(2)	Space group: $P\bar{1}$
b(Å): 18.946(3)	Cell volume (Å^3): 914.7(4)
c(Å): 6.986(1)	Cell content: $4[Na(Ca,R.E.)_2Si_4O_{10}F]$
α(°): 89.88(2)	D_m: 2.902 g cm^{-3}
β(°): 116.65(2)	D_c: 2.887 g cm^{-3}
γ(°): 94.34(2)	μ(Mo$K\alpha$): 18.20 cm^{-1}

The combination of 5 symbols yielded 32 solutions. Four E-maps appeared equally probable, out of which one showed a geometrically better view of the structure. From this E-map, positions of 4 Ca, 7 Si, 1 F, and 14 O atoms were determined. Two cycles of structure-factor calculations followed by difference Fourier syntheses yielded the positions of all the missing Na, Si, O, and F atoms. A few cycles of refinement using the isotropic temperature factors reduced the R factor to 0.086 from an initial value of 0.40. The isotropic temperature factor for Ca(1A) turned out to be negative, indicating partial occupancy of this site by the rare-earth atoms. A difference Fourier synthesis also indicated positive electron densities at the Ca sites. Hence, a site-occupancy refinement of the calcium and rare-earth atoms was carried out, using the full-matrix least-squares program RFINE (Finger, 1969). The scattering factor for the rare-earth atoms was approximated by averaging the scattering factors of the rare-earth atoms in the chemical analysis reported by Gittins *et al.* (1976). The site-occupancy refinement indicated most of the rare-earth atoms to be concentrated in the Ca(1A) site; the temperature factor for Ca(1A) became positive. The R factor at this stage was 0.076.

Since the number of variable parameters was too large, the final least-squares refinement of the structure using anisotropic temperature factors was carried out by the program CRYLSQ (Stewart *et al.*, 1972) in blocks, one block being assigned to each atom. The atomic scattering factors for Na, Ca, RE, Si, O, and F were taken from Cromer and Mann (1968) and corrected for anomalous dispersion (Cromer and Liberman, 1970). The observed structure factors (Fo's) were weighted by the formula $1/\sigma^2(F\text{o})$, where $\sigma(F\text{o})$ is the standard deviation of the measurement of Fo, as determined from the counting statistics.

Table 2. Agrellite: positional and thermal parameters and site occupancies (with standard deviations in parentheses)

Atom	x	y	z	u	u_{11}	u_{22}	u_{33}	u_{12}	u_{13}	u_{23}
Ca(1A)	0.99796(14)	0.21554(5)	0.99620(15)	1.16(3)	165(5)	93(4)	90(3)	-0(4)	72(3)	25(3)
Ca(1B)	0.54176(12)	0.28461(4)	0.01966(13)	0.92(3)	142(4)	76(4)	83(4)	3(3)	66(3)	18(3)
Ca(2A)	0.45521(12)	0.72007(4)	0.48010(13)	0.94(3)	133(4)	85(4)	89(4)	1(3)	71(3)	21(3)
Ca(2B)	0.00155(13)	0.78166(5)	0.50022(14)	1.27(3)	194(4)	101(4)	124(4)	14(3)	108(3)	27(3)
Na(A)	0.23539(28)	0.99102(11)	0.86794(34)	2.49(7)	151(9)	287(12)	286(11)	5(8)	80(8)	29(9)
Na(B)	0.26104(29)	0.50234(12)	0.13576(36)	2.84(8)	139(9)	370(13)	331(12)	-3(9)	74(9)	40(10)
Si(1A)	0.20870(16)	0.93103(6)	0.35569(17)	0.81(3)	106(5)	69(5)	76(5)	8(4)	51(4)	27(4)
Si(1B)	0.30739(16)	0.56807(6)	0.65542(18)	0.79(3)	105(5)	70(5)	83(5)	12(4)	54(4)	28(4)
Si(2A)	0.48573(16)	0.87795(6)	0.21377(17)	0.80(4)	108(5)	82(5)	63(5)	-1(4)	56(4)	20(4)
Si(2B)	0.02460(16)	0.61933(6)	0.79397(17)	0.75(4)	93(5)	78(5)	74(5)	-0(4)	46(4)	18(4)
Si(3A)	0.16705(16)	0.08998(6)	0.33394(17)	0.78(3)	92(5)	77(5)	74(5)	5(4)	48(4)	23(4)
Si(3B)	0.67404(16)	0.59022(6)	0.34109(17)	0.75(3)	87(5)	70(5)	85(5)	6(4)	45(4)	21(4)
Si(4A)	0.48619(16)	0.87771(6)	0.77347(18)	0.80(4)	107(5)	75(5)	68(5)	-4(4)	55(4)	21(4)
Si(4B)	0.02139(16)	0.61974(6)	0.23430(18)	0.72(4)	94(5)	81(5)	67(5)	2(4)	50(4)	23(4)
F(A)	0.7607(4)	0.7610(2)	0.1268(5)	2.7(1)	170(14)	243(17)	423(19)	-2(12)	117(13)	82(14)
F(B)	0.2353(4)	0.2451(2)	0.3595(5)	2.5(1)	180(14)	223(16)	356(17)	-3(12)	69(13)	3(13)
O(1A)	0.3493(4)	0.9351(2)	0.6138(5)	1.3(1)	167(15)	117(15)	79(13)	8(11)	32(11)	29(11)
O(1B)	0.1641(4)	0.5639(2)	0.3974(5)	1.3(1)	170(15)	111(15)	85(13)	35(11)	28(11)	38(11)
O(2A)	0.1028(4)	0.0048(1)	0.3023(5)	1.1(1)	143(14)	77(14)	122(14)	19(11)	76(11)	29(11)
O(2B)	0.5891(4)	0.5065(1)	0.2960(5)	1.0(1)	107(14)	66(13)	148(14)	13(10)	58(11)	26(11)
O(3A)	0.3483(4)	0.9352(2)	0.2356(5)	1.2(1)	182(15)	115(15)	153(15)	24(11)	135(12)	24(11)
O(3B)	0.1722(4)	0.5640(2)	0.7804(5)	1.3(1)	155(14)	124(15)	176(15)	38(11)	131(12)	28(12)
O(4A)	0.0620(4)	0.8634(2)	0.2822(5)	1.3(1)	163(15)	109(15)	141(14)	-14(11)	96(12)	11(11)
O(4B)	0.4543(4)	0.6355(1)	0.7256(5)	1.1(1)	136(14)	98(14)	106(13)	-12(11)	64(11)	19(11)
O(5A)	0.3938(4)	0.7990(1)	0.1901(5)	1.1(1)	192(15)	87(14)	78(13)	-28(11)	90(11)	3(11)
O(5B)	0.1102(4)	0.6991(2)	0.8169(5)	1.4(1)	126(14)	91(14)	176(15)	0(11)	58(12)	34(11)
O(6A)	0.5130(4)	0.9064(1)	0.0072(4)	1.1(1)	177(15)	105(15)	74(13)	-15(11)	82(11)	21(11)
O(6B)	0.9958(4)	0.5913(2)	0.0012(5)	1.2(1)	172(15)	161(16)	91(14)	-5(12)	84(12)	3(12)
O(7A)	0.7013(4)	0.8924(2)	0.4117(5)	1.6(1)	140(15)	210(17)	107(14)	-8(12)	33(12)	-11(12)
O(7B)	0.8136(4)	0.6001(2)	0.5964(5)	1.5(1)	143(15)	179(16)	96(14)	6(12)	20(11)	-8(12)
O(8A)	0.9743(4)	0.1295(2)	0.2368(5)	1.1(1)	114(13)	113(14)	130(14)	45(11)	60(11)	61(11)
O(8B)	0.4984(4)	0.6382(2)	0.2562(5)	1.2(1)	133(14)	113(15)	103(14)	53(11)	48(11)	42(11)
O(9A)	0.7019(4)	0.8922(2)	0.7911(5)	1.6(1)	153(15)	215(17)	147(15)	4(12)	108(12)	45(13)
O(9B)	0.8079(4)	0.6032(2)	0.2180(5)	1.5(1)	136(14)	178(16)	203(16)	5(12)	123(13)	62(13)
O(10A)	0.3947(4)	0.7986(1)	0.7067(5)	1.3(1)	193(15)	77(14)	119(14)	2(11)	92(12)	12(11)
O(10B)	0.1082(4)	0.6993(1)	0.2962(5)	1.2(1)	128(14)	80(14)	143(14)	-24(11)	60(11)	12(11)

Site	Ca	R.E.	Site	Ca	R.E.
Ca(1A)	0.8534	0.1466(6)	Ca(1B)	0.978	0.022(2)
Ca(2A)	0.993	0.007(2)	Ca(2B)	0.985	0.015(2)

Form of the anisotropic temperature factor (x10^2): $exp[-2\pi^2(u_{11}h^2a^{*2} + u_{22}k^2b^{*2} + u_{33}l^2c^{*2} + 2u_{12}hka^*b^*\cos\gamma^* + 2u_{13}hla^*c^*\cos\beta^* + 2u_{23}klb^*c^*\cos\alpha^*)]$.

Five cycles of refinement reduced the R factor to the final value of 0.045 for 5343 reflections. The final occupancy factors, positional and thermal parameters are given in Table 2 and a list of observed and calculated structure factors in Table 3[1]. Bond lengths and angles (Tables 4, 5, and 6) have been calculated using the program BONDLA (Stewart *et al.*, 1972). The estimated standard deviations in bond lengths and angles include the standard deviations of the measurement of the unit-cell dimensions. The average deviations in Na–O, Ca–O, and Si–O bond lengths are 0.004, 0.003, and 0.003A, and in O–Na–O, O–Ca–O and O–Si–O angles 0.1, 0.1, and 0.2° respectively.

[1] To obtain a copy of this table, order Document AM-79-101 from the Business Office, Mineralogical Society of America, 2000 Florida Ave., N.W., Washington, D.C. 20009. Please remit $1.00 in advance for the microfiche.

Pseudosymmetry and atom nomenclature

Gittins *et al.* (1976) proposed an alternative pseudomonoclinic C-centered unit cell for agrellite, with double the volume of the triclinic cell. We note a strong tendency towards C-centering in terms of the

Table 4. Agrellite: interatomic distances (A) and angles (°) within the Ca-polyhedra (with standard deviations in parentheses)

The Ca(1A) Polyhedron		*The Ca(2B) Polyhedron*	
Ca(1A)-F(A)	2.400(4)	Ca(2B)-F(A)	2.444(3)
Ca(1A)-F(B)	2.409(3)	Ca(2B)-F(B)	2.464(4)
Ca(1A)-O(4A)	2.309(3)	Ca(2B)-O(4A)	2.337(4)
Ca(1A)-O(5A)	2.708(3)	Ca(2B)-O(10A)	2.720(3)
Ca(1A)-O(5B)	2.495(4)	Ca(2B)-O(5B)	2.562(3)
Ca(1A)-O(8A)	2.395(4)	Ca(2B)-O(8A)	2.430(4)
Ca(1A)-O(9A)	3.066(3)	Ca(2B)-O(7A)	3.107(4)
Ca(1A)-O(10B)	2.476(3)	Ca(2B)-O(10B)	2.532(4)
Mean of 2Ca-F distances	2.405		2.454
Mean of 6Ca-O distances	2.575		2.615
O(5A)-O(4A)	3.239(5)	O(10A)-O(4A)	3.250(4)
O(5A)-O(10B)	3.141(5)	O(10A)-O(10B)	3.221(4)
O(5A)-O(5B)	3.077(4)	O(10A)-O(5B)	3.148(5)
O(5A)-O(8A)	3.436(5)	O(10A)-O(8A)	3.439(4)
O(4A)-O(10B)	3.152(4)	O(4A)-O(10B)	3.152(4)
O(10B)-O(5B)	3.356(5)	O(10B)-O (5B)	3.631(4)
O(5B)-O(8A)	3.348(4)	O(5B)-O(8A)	3.348(4)
O(8A)-O(4A)	3.513(5)	O(8A)-O(4A)	3.501(5)
F(B) -F(A)	3.415(4)	F(A) -F(B)	3.578(4)
F(A) -O(9A)	3.329(5)	F(A) -O(7A)	3.374(5)
O(9A)-F(B)	2.963(5)	F(B) -O(7A)	3.009(5)
F(B) -O(5B)	2.699(4)	F(B) -O(5B)	2.699(4)
F(B) -O(8A)	2.723(4)	F(B) -O(8A)	2.723(4)
O(9A)-O(8A)	2.667(5)	O(7A)-O(8A)	2.673(4)
O(9A)-O(4A)	3.391(5)	O(7A)-O(4A)	3.386(6)
F(A) -O(4A)	2.730(4)	F(A) -O(4A)	2.730(4)
F(A) -O(10B)	2.765(4)	F(A) -O(10B)	2.765(4)
F(A)-Ca(1A)-F(B)	90.5(1)	F(A)-Ca(2B)-F(B)	93.6(1)
F(A)-Ca(1A)-O(4A)	70.8(1)	F(A)-Ca(2B)-O(4A)	69.6(1)
F(A)-Ca(1A)-O(5A)	135.5(1)	F(A)-Ca(2B)-O(10A)	134.7(1)
F(A)-Ca(1A)-O(5B)	127.0(1)	F(A)-Ca(2B)-O(5B)	130.7(1)
F(A)-Ca(1A)-O(8A)	130.8(1)	F(A)-Ca(2B)-O(8A)	129.9(1)
F(A)-Ca(1A)-O(10B)	69.1(1)	F(A)-Ca(2B)-O(10B)	67.5(1)
F(B)-Ca(1A)-O(4A)	140.3(1)	F(B)-Ca(2B)-O(4A)	139.3(1)
F(B)-Ca(1A)-O(5A)	131.9(1)	F(B)-Ca(2B)-O(10A)	130.5(1)
F(B)-Ca(1A)-O(5B)	66.8(1)	F(B)-Ca(2B)-O(5B)	64.9(1)
F(B)-Ca(1A)-O(8A)	69.0(1)	F(B)-Ca(2B)-O(8A)	67.6(1)
F(B)-Ca(1A)-O(9A)	64.2(1)	F(B)-Ca(2B)-O(7A)	64.2(1)
F(B)-Ca(1A)-O(10B)	124.2(1)	F(B)-Ca(2B)-O(10B)	128.1(1)
O(4A)-Ca(1A)-O(5A)	80.0(1)	O(4A)-Ca(2B)-O(10A)	79.6(1)
O(4A)-Ca(1A)-O(5B)	151.8(1)	O(4A)-Ca(2B)-O(5B)	152.6(1)
O(4A)-Ca(1A)-O(8A)	96.6(1)	O(4A)-Ca(2B)-O(8A)	94.5(1)
O(4A)-Ca(1A)-O(9A)	76.8(1)	O(4A)-Ca(2B)-O(7A)	75.4(1)
O(4A)-Ca(1A)-O(10B)	82.3(1)	O(4A)-Ca(2B)-O(10B)	80.6(1)
O(5A)-Ca(1A)-O(5B)	72.4(1)	O(10A)-Ca(2B)-O(5B)	73.1(1)
O(5A)-Ca(1A)-O(8A)	84.4(1)	O(10A)-Ca(2B)-O(8A)	83.6(1)
O(5A)-Ca(1A)-O(9A)	131.3(1)	O(10A)-Ca(2B)-O(7A)	129.7(1)
O(5A)-Ca(1A)-O(10B)	74.4(1)	O(10A)-Ca(2B)-O(10B)	75.6(1)
O(5B)-Ca(1A)-O(8A)	86.4(1)	O(5B)-Ca(2B)-O(8A)	84.2(1)
O(5B)-Ca(1A)-O(9A)	126.4(1)	O(5B)-Ca(2B)-O(7A)	124.1(1)
O(5B)-Ca(1A)-O(10B)	84.9(1)	O(5B)-Ca(2B)-O(10B)	90.9(1)
O(8A)-Ca(1A)-O(9A)	56.9(1)	O(8A)-Ca(2B)-O(7A)	56.2(1)
O(8A)-Ca(1A)-O(10B)	158.7(1)	O(8A)-Ca(2B)-O(10B)	159.1(1)
O(9A)-Ca(1A)-O(10B)	141.7(1)	O(7A)-Ca(2B)-O(10B)	139.6(1)
The Ca(2A) Polyhedron		*The Ca(1B) Polyhedron*	
Ca(2A) - F(B)	2.192(3)	Ca(1B) - F(A)	2.201(3)
Ca(2A) - O(4B)	2.346(3)	Ca(1B) - O(4B)	2.326(3)
Ca(2A) - O(5A)	2.408(3)	Ca(1B) - O(5A)	2.387(4)
Ca(2A) - O(8B)	2.350(4)	Ca(1B) - O(8B)	2.338(3)
Ca(2A) - O(10A)	2.392(4)	Ca(1B) - O(10A)	2.376(3)
Ca(2A) - O(10B)	2.407(3)	Ca(1B) - O(5B)	2.408(3)
Mean of 5Ca-O distances	2.381		2.367
F(B) - O(4B)	3.424(5)	F(A) - O(4B)	3.515(4)
F(B) - O(5A)	3.335(5)	F(A) - O(10A)	3.163(4)
F(B) - O(8B)	3.275(4)	F(A) - O(5A)	3.203(5)
F(B) - O(10A)	3.270(5)	F(A) - O(8B)	3.361(5)
O(10B) - O(4B)	3.305(4)	O(5B) - O(4B)	3.317(5)
O(10B) - O(8B)	3.446(5)	O(5B) - O(10A)	3.148(5)
O(10B) - O(5A)	3.141(5)	O(5B) - O(5A)	3.077(4)
O(10B) - O(10A)	3.221(4)	O(5B) - O(8B)	3.470(4)
O(4B) - O(8B)	3.446(5)	O(4B) - O(10A)	3.152(4)
O(8B) - O(5A)	3.192(4)	O(10A) - O(5A)	3.380(5)
O(5A) - O(10A)	3.606(5)	O(5A) - O(8B)	3.192(4)
O(10A) - O(4B)	3.152(4)	O(8B) - O(4B)	3.446(5)
F(B)-Ca(2A)-O(4B)	97.9(1)	F(A)-Ca(1B)-O(4B)	101.8(1)
F(B)-Ca(2A)-O(5A)	92.8(1)	F(A)-Ca(1B)-O(5A)	88.5(1)
F(B)-Ca(2A)-O(8B)	92.2(1)	F(A)-Ca(1B)-O(8B)	95.5(1)
F(B)-Ca(2A)-O(10A)	90.9(1)	F(A)-Ca(1B)-O(10A)	87.4(1)
F(B)-Ca(2A)-O(10B)	171.9(10)	F(A)-Ca(1B)-O(5B)	164.3(1)
O(4B)-Ca(2A)-O(5A)	169.3(1)	O(4B)-Ca(1B)-O(5A)	168.1(1)
O(4B)-Ca(2A)-O(8B)	94.4(1)	O(4B)-Ca(1B)-O(8B)	99.7(1)
O(4B)-Ca(2A)-O(10A)	83.4(1)	O(4B)-Ca(1B)-O(10A)	84.2(1)
O(4B)-Ca(2A)-O(10B)	88.1(1)	O(4B)-Ca(1B)-O(5B)	88.9(1)
O(5A)-Ca(2A)-O(8B)	84.2(1)	O(5A)-Ca(1B)-O(8B)	85.0(1)
O(5A)-Ca(2A)-O(10A)	97.4(1)	O(5A)-Ca(1B)-O(10A)	90.4(1)
O(5A)-Ca(2A)-O(10B)	81.4(1)	O(5A)-Ca(1B)-O(5B)	79.8(1)
O(8B)-Ca(2A)-O(10A)	176.5(1)	O(8B)-Ca(1B)-O(10A)	174.5(1)
O(8B)-Ca(2A)-O(10B)	92.8(1)	O(8B)-Ca(1B)-O(5B)	93.9(1)
O(10A)-Ca(2A)-O(10B)	84.3(1)	O(10A)-Ca(1B)-O(5B)	82.3(1)

Table 5. Agrellite: interatomic distances (A) and angles (°) within the Na-polyhedra (with standard deviations in parentheses)

The Na(A)- and Na(B)- Polyhedra					
	A	B		A	B
Na-O(1)	2.571(5)	2.578(5)	O(1)-Na-O(2)	110.5(1)	106.9(1)
Na-O(2)	2.353(4)	2.270(4)	O(1)-Na-O(3)	115.5(1)	115.1(1)
Na-O(3)	2.568(4)	2.564(4)	O(1)-Na-O(6)	58.6(1)	59.0(1)
Na-O(6)	2.606(4)	2.597(4)	O(1)-Na-O(6′)	95.9(1)	98.8(1)
Na-O(6′)	2.501(3)	2.408(4)	O(1)-Na-O(7)	70.8(1)	69.3(1)
Na-O(7)	3.102(4)	2.897(4)	O(1)-Na-O(8)	78.7(1)	75.2(1)
Na-O(8)	2.603(4)	2.937(4)	O(1)-Na-O(9)	148.8(1)	153.2(1)
Na-O(9)	3.102(4)	3.011(4)	O(2)-Na-O(3)	110.9(2)	104.7(2)
Mean	2.676	2.658	O(2)-Na-O(6)	144.1(1)	137.7(1)
			O(2)-Na-O(6′)	127.3(1)	134.7(1)
O(1)-O(6)	2.536(4)	2.548(4)	O(2)-Na-O(7)	93.1(1)	98.8(1)
O(1)-O(7)	3.317(5)	3.125(5)	O(2)-Na-O(8)	62.9(1)	58.9(1)
O(1)-O(8)	3.281(5)	3.379(4)	O(2)-Na-O(9)	93.5(1)	96.8(1)
O(2)-O(7)	2.634(4)	2.617(4)	O(3)-Na-O(6)	58.6(1)	59.3(1)
O(2)-O(8)	2.593(4)	2.624(4)	O(3)-Na-O(6′)	95.9(1)	96.9(1)
O(2)-O(9)	2.638(5)	2.624(5)	O(3)-Na-O(7)	148.8(1)	152.9(1)
O(3)-O(6)	2.532(6)	2.554(4)	O(3)-Na-O(8)	78.9(1)	75.2(1)
O(3)-O(8)	3.286(4)	3.371(4)	O(3)-Na-O(9)	70.9(1)	69.1(1)
O(3)-O(9)	3.317(5)	3.183(5)	O(6)-Na-O(6′)	88.6(1)	87.6(1)
O(6)-O(6′)	3.567(4)	3.568(4)	O(6)-Na-O(7)	111.8(1)	110.0(1)
O(6′)-O(7)	4.735(4)	4.963(6)	O(6)-Na-O(8)	81.2(1)	78.8(1)
O(6′)-O(9)	2.559(6)	2.550(6)	O(6)-Na-O(9)	111.7(1)	110.2(1)
			O(6′)-Na-O(7)	53.0(1)	56.4(1)
			O(6′)-Na-O(8)	169.8(1)	166.4(1)
			O(6′)-Na-O(9)	53.0(1)	54.8(1)
			O(7)-Na-O(8)	131.2(2)	129.6(1)
			O(7)-Na-O(9)	88.7(1)	95.2(1)
			O(8)-Na-O(9)	131.5(1)	129.3(1)

measured X-ray intensities based on the triclinic unit cell. This pseudo-C-centering is clearly manifest in terms of the positional parameters of all the atoms, except fluorine. The atoms so related have been designated as A and B (Table 2). The sodium polyhedra and silicate tetrahedra occur in pairs, which are nearly identical in stereochemical configuration (Tables 5, 6). However, due to the considerable deviation of the fluorine atoms from their true C-centered positions, the calcium atoms, related by the pseudo-C-centering operation, have different types of coordination polyhedra, although they also occur in pairs with nearly identical configurations (Table 4).

Description of the structure

The crystal structure of agrellite consists of (a) silicate tubes crosslinked by sodium atoms into sodium silicate layers, and (b) calcium polyhedral layers, both parallel to the (010) plane, alternating along the *b* axis to form a three-dimensional framework.

The silicate tubes

The silicate tube consists of two centrosymmetrically-related single silicate chains; each single chain is formed by corner-sharing four-membered tetrahedral rings [Si(1)–Si(2)–Si(3)–Si(4) in Figs. 1a,b] and is the same as the $[Si_4O_{11}]$ chain found in vlasovite, $Na_2ZrSi_4O_{11}$ (Voronkov and Pyatenko, 1961; Fleet and Cann, 1967). Within each chain two tetrahedra of the four-membered ring point up and two down along the *b* axis. Two centrosymmetrically-related chains are connected by sharing opposing tetrahedral corners, giving rise to a silicate tube with the compo-

Table 6. Agrellite: Si–O bond distances (A) and angles (°) (with standard deviations in parentheses)

The Si(1A)- and Si(1B)- Tetrahedra

	A	B		A	B
Si(1)-O(1)	1.634(3)	1.637(3)	O(1)-Si(1)-O(2)	105.6(2)	104.8(2)
Si(1)-O(2)	1.633(3)	1.638(3)	O(1)-Si(1)-O(3)	107.5(2)	108.0(2)
Si(1)-O(3)	1.639(4)	1.637(4)	O(1)-Si(1)-O(4)	112.6(2)	112.3(2)
Si(1)-O(4)	1.568(3)	1.567(3)	O(2)-Si(1)-O(3)	105.3(2)	105.2(2)
Mean	1.619	1.620	O(2)-Si(1)-O(4)	113.1(2)	113.7(2)
			O(3)-Si(1)-O(4)	112.1(2)	112.3(2)
O(1)-O(2)	2.603(4)	2.595(4)	Mean	109.4	109.4
O(1)-O(3)	2.639(5)	2.648(5)			
O(1)-O(4)	2.665(4)	2.662(4)			
O(2)-O(3)	2.602(5)	2.601(5)			
O(2)-O(4)	2.671(4)	2.684(4)			
O(3)-O(4)	2.661(5)	2.661(5)			
Mean	2.640	2.642			

The Si(2A)- and Si(2B)- Tetrahedra

	A	B		A	B
Si(2)-O(3)	1.630(4)	1.643(4)	O(3)-Si(2)-O(5)	112.3(2)	112.0(2)
Si(2)-O(5)	1.583(3)	1.583(3)	O(3)-Si(2)-O(6)	101.8(2)	102.1(2)
Si(2)-O(6)	1.634(4)	1.642(4)	O(3)-Si(2)-O(7)	108.5(2)	108.0(2)
Si(2)-O(7)	1.625(3)	1.613(3)	O(5)-Si(2)-O(6)	115.3(2)	114.5(2)
Mean	1.618	1.620	O(5)-Si(2)-O(7)	114.4(2)	116.3(2)
			O(6)-Si(2)-O(7)	103.4(2)	102.8(2)
O(3)-O(5)	2.668(4)	2.674(5)	Mean	109.3	109.3
O(3)-O(6)	2.532(6)	2.554(6)			
O(3)-O(7)	2.642(4)	2.634(4)			
O(5)-O(6)	2.718(5)	2.712(5)			
O(5)-O(7)	2.697(4)	2.714(4)			
O(6)-O(7)	2.558(4)	2.544(4)			
Mean	2.636	2.639			

The Si(3A)- and Si(3B)- Tetrahedra

	A	B		A	B
Si(3)-O(2)	1.637(3)	1.645(3)	O(2)-Si(3)-O(7)	107.8(2)	106.6(2)
Si(3)-O(7)	1.623(3)	1.621(3)	O(2)-Si(3)-O(8)	107.1(2)	108.9(2)
Si(3)-O(8)	1.585(3)	1.580(3)	O(2)-Si(3)-O(9)	107.7(2)	106.8(2)
Si(3)-O(9)	1.629(4)	1.625(4)	O(7)-Si(3)-O(8)	112.8(2)	113.9(2)
Mean	1.619	1.618	O(7)-Si(3)-O(9)	109.0(2)	107.9(2)
			O(8)-Si(3)-O(9)	112.1(2)	112.4(2)
O(2)-O(7)	2.634(4)	2.617(4)	Mean	109.4	109.4
O(2)-O(8)	2.593(4)	2.624(4)			
O(2)-O(9)	2.638(5)	2.624(5)			
O(7)-O(8)	2.673(4)	2.683(4)			
O(7)-O(9)	2.648(5)	2.624(5)			
O(8)-O(9)	2.667(5)	2.663(5)			
Mean	2.642	2.639			

The Si(4A)- and Si(4B)- Tetrahedra

	A	B		A	B
Si(4)-O(1)	1.631(3)	1.638(3)	O(1)-Si(4)-O(6)	101.7(2)	102.2(2)
Si(4)-O(6)	1.639(4)	1.637(4)	O(1)-Si(4)-O(9)	108.4(2)	107.7(1)
Si(4)-O(9)	1.624(4)	1.615(4)	O(1)-Si(4)-O(10)	112.6(2)	112.3(1)
Si(4)-O(10)	1.585(3)	1.582(3)	O(6)-Si(4)-O(9)	103.3(2)	103.3(2)
Mean	1.620	1.618	O(6)-Si(4)-O(10)	115.4(2)	114.5(2)
O(1)-O(6)	2.536(4)	2.548(4)	O(9)-Si(4)-O(10)	114.4(2)	114.9(2)
O(1)-O(9)	2.640(4)	2.639(4)	Mean	109.3	109.2
O(1)-O(10)	2.676(4)	2.674(4)			
O(6)-O(9)	2.559(6)	2.5550(6)			
O(6)-O(10)	2.725(4)	2.707(4)			
O(9)-O(10)	2.698(4)	2.695(4)			
Mean	2.639	2.636			

Si-Si distances / *Si-O-Si angles*

	A	B		A	B
Si(1)-Si(2)	2.976(2)	2.988(2)	Si(1)-O(1)-Si(4)	131.3(2)	132.7(2)
Si(1)-Si(3)	3.049(2)	3.013(2)	Si(1)-O(2)-Si(3)	137.6(2)	133.2(2)
Si(1)-Si(4)	2.976(2)	3.000(2)	Si(1)-O(2)-Si(3)	137.6(2)	133.2(2)
Si(2)-Si(3)	3.129(2)	3.126(2)	Si(2)-O(6)-Si(4)	140.2(2)	140.7(2)
Si(2)-Si(4)	3.078(2)	3.088(2)	Si(2)-O(7)-Si(3)	147.7(3)	150.3(3)
Si(3)-Si(4)	3.120(2)	3.116(2)	Si(3)-O(9)-Si(4)	147.1(2)	148.2(2)
			Mean	139.2	139.4

sition $[Si_8O_{20}]$, whose diameter is defined by a basket-shaped six-membered ring [Si(2)–Si(3)–Si(1)–Si(4)–Si(3′)–Si(1′) in Figs. 1a,b]. In addition each tube contains two different boat-shaped eight-membered tetrahedral rings [Si(1)–Si(4)–Si(2)–Si(1′)–Si(3)–Si(4′)–Si(2′)–Si(3′) and Si(3)–Si(4)–Si(2)–Si(3′)–Si(1)–Si(4′)–Si(2′)–Si(1′) in Figs. 1a,b], which have four tetrahedra in common. There are two crystallographically-distinct silicate tubes (A and B), whose configurations are only slightly different from each other. These silicate tubes run parallel to the *c* axis and are hexagonally close-packed in the (001) plane (Fig. 2).

The sodium silicate layers

The silicate tubes occur in layers parallel to the (010) plane. Within each layer they are packed in a staggered fashion, leaving cavities at the boat-shaped eight-membered rings. The sodium atoms occur within these cavities in eight-fold coordination (Figs. 3a,b). The $Na(A)O_8$ and $Na(B)O_8$ polyhedra are distorted cubes with very similar configurations; the average Na–O distances are 2.676 and 2.658A respectively. Within these two polyhedra, the average variation in corresponding Na–O bond lengths and O–Na–O angles are 0.083A and 3.1° respectively (Table 5). Each sodium polyhedron shares six corners with the silicate tube below and two with the silicate tube above. In addition, two sodium polyhedra occurring on either side of a silicate tube share a polyhedral edge [O(6)–O(6′)], thereby forming a dimer. Two crystallographically distinct sodium silicate layers (*A* and *B*), parallel to the (010) plane, with very similar stereochemical configurations are formed this way (Figs. 3a,b).

The calcium polyhedral layers

Both calcium atoms, Ca(1A) and Ca(2B), are coordinated to six oxygen and two fluorine atoms each. The irregular coordination polyhedron consists of two parts, (a) a square-pyramid formed by five oxygen atoms, and (b) two fluorine atoms and an oxygen atom at the corners of a triangle occurring above the equatorial plane (Fig. 4). Within the $Ca(1A)O_6F_2$ and $Ca(2B)O_6F_2$ polyhedra, the averages of 6 Ca–O distances are 2.575 and 2.615A and the averages of two Ca–F distances are 2.405 and 2.454A respectively. The Ca(1A) site contains most of the rare-earth ions (Table 2). The Ca(2B) polyhedron is slightly larger than the Ca(1A) polyhedron; hence the former site may be slightly too large to contain a large fraction of the rare-earth ions. The corresponding O–Ca–O or O–Ca–F angles within the Ca(1A) and Ca(2B) polyhedra are very similar (av. deviation 1.7°) (Table 4). Both Ca(2A) and Ca(1B) are surrounded by five oxygen and one fluorine atoms each at the corners of distorted octahedra; the averages of five Ca–O distances are 2.381 and 2.367A, and the Ca–F distances 2.192 and 2.201A, respectively.

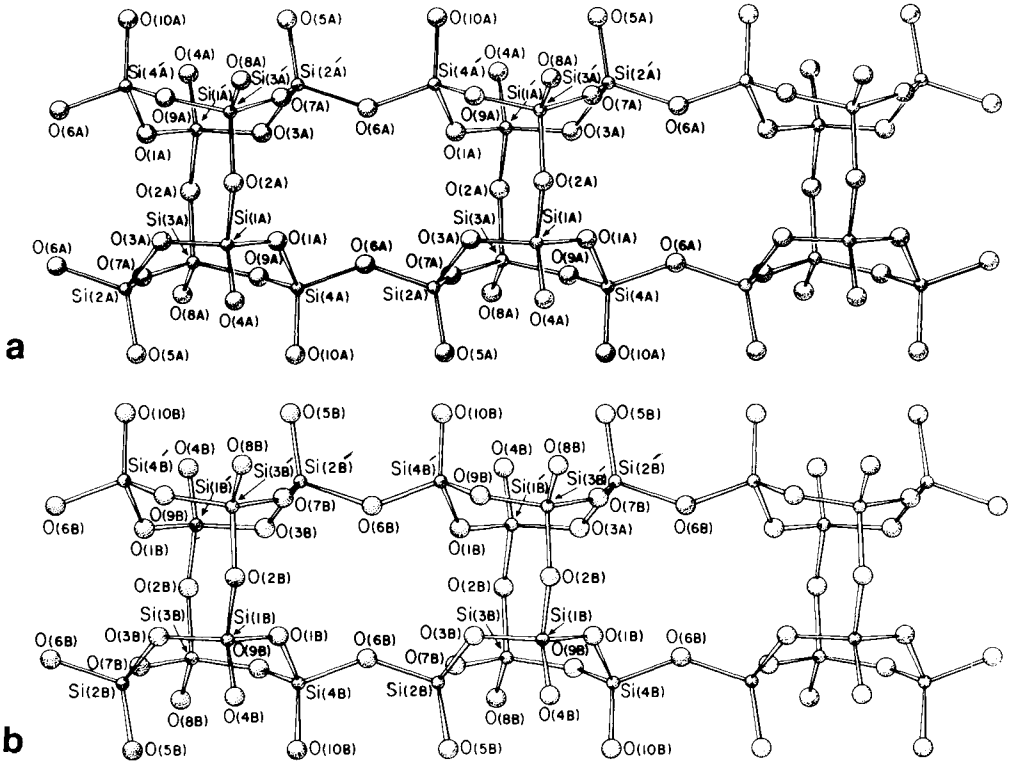

Fig. 1a,b. Agrellite: stereochemical configuration of the two crystallographically different $[Si_8O_{20}]$ double chains (tubes) A and B.

Again, the O–Ca–O and O–Ca–F angles within these two octahedra are remarkably similar (av. deviation 3.0°) (Table 4). The Ca(2A) and Ca(1B) sites contain very small amounts of the rare-earth ions, which is consistent with their smaller polyhedral sizes.

Alternating Ca(1A) and Ca(2B) polyhedra share opposite triangular faces [F(A)–O(4A)–O(10B) and F(B)–O(5B)–O(8A)]; likewise, Ca(2A) and Ca(1B) octahedra share opposite octahedral edges [O(4B)–O(10A) and O(5A)–O(8B)], thereby forming two different polyhedral chains parallel to the *c* axis, which alternate along the *a* axis. Furthermore, the Ca(1A) and Ca(2B) polyhedra share square-pyramidal edges with the octahedral edges [O(5A)–O(10B), O(10B)–O(10A), O(10A)–O(5B), and O(5B)–O(5A)] of the Ca(2A) and Ca(1B) octahedra, which result in a polyhedral layer parallel to the (010) plane (Fig. 4).

The three-dimensional framework

If we designate the calcium polyhedral layer as *C* and its centrosymmetric equivalent as $\bar{C}$, and the two different sodium silicate layers as *A* and *B*, the stacking sequence of the layers along the *b* axis is: $AC\bar{B}\bar{C}A\bar{C}B\bar{C}\cdots$. The configuration of the oxygen atoms on one side of the calcium polyhedral layer (set of A oxygens) is slightly different from those occurring on the other side (set of B oxygens). The sodium silicate layer, *A*, occurs in between two sets of A-layer oxygen atoms, whereas the sodium silicate layer, *B*, occurs in between two sets of B-layer oxygen atoms. The sodium silicate layers are connected to the calcium polyhedral layers by sharing silicate tetrahedral corners with the calcium polyhedral corners (Fig. 5).

Stereochemical configuration of the silicate double chain (tube) $[Si_8O_{20}]^{8-}$

The Si–O bond lengths and Si–O–Si angles

The average Si–O distances within the eight crystallographically-different silicate tetrahedra are remarkably constant, with a value of 1.619±0.001A. The angular distortions within the individual tetrahedra are comparable; the O–Si–O angles vary from 101.7 to 116.3° (Table 6).

If we ignore the very long Ca–O or Na–O bonds (>3.0A), the oxygen atoms can be divided into five groups in terms of coordination:

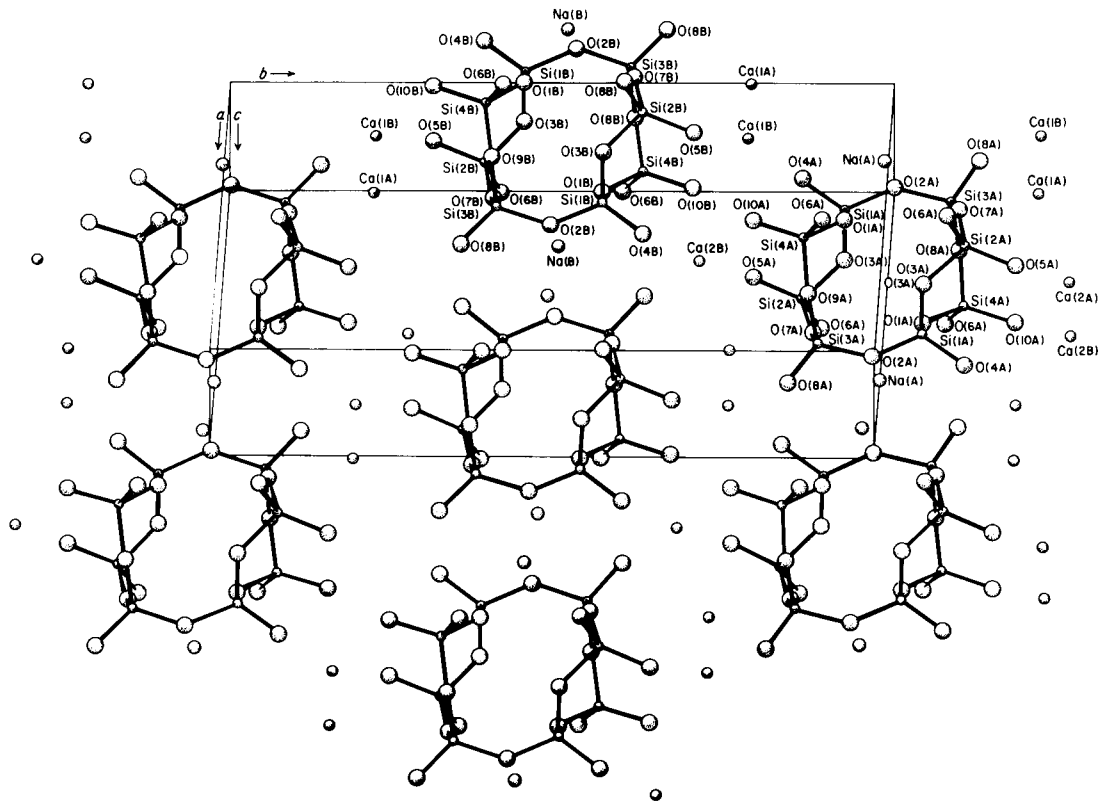

Fig. 2. Agrellite: projection of the silicate tubes parallel to the c axis; note the hexagonal close-packing of the tubes in the (001) plane.

Oxygen type	Av. Si–O bond length (A)	Av. Si–O–Si angle(°)
A: 1Si + 3(Ca,Na)	1.583	—
B: 1Si + 2Ca	1.568	—
C: 2Si + 2Na	1.636	140.5
D: 2Si + 1Na	1.637	132.9
E: 2Si only	1.622	148.3

Within each silicate tetrahedron, there is one non-bridging and three bridging Si–O bonds. As expected, the non-bridging Si–O bonds (Types A and B) are significantly shorter than the bridging Si–O bonds (Types C, D, E). Since the B-type oxygen atoms are bonded to two calcium atoms each in addition to one silicon atom, they are charge-deficient as opposed to the A-type oxygen atoms, each of which is bonded to three calcium and one silicon atoms. As a result, the B-type Si–O bonds (av. 1.568A) are significantly shorter than the A-type Si–O bonds (av. 1.583A). Within the bridging Si–O bonds, the E-type bonds (av. 1.622A) are significantly shorter than the C- and D-types (av. 1.636 and 1.637A), which are nearly identical. The E-type bonds are also associated with larger Si–O–Si angles (av. 148.3°) than those associated with C- and D-type bonds (140.5 and 132.9° respectively).

A correlation of the larger Si–O–Si angles with the shorter Si–O bond lengths and *vice versa* has been found through the molecular orbital calculations on silicate chain fragments (Tossell and Gibbs, 1977). Similar correlation has been observed in rosenhahnite, $Ca_3Si_3O_8(OH)_2$ (Wan *et al.*, 1977), zektzerite, $NaLiZrSi_6O_{15}$ (Ghose and Wan, 1978b) and inesite, $Ca_2Mn_7Si_{10}O_{28}(OH)_2 \cdot 5H_2O$ (Wan and Ghose, 1978).

Comparison with related structures

Silicate tubes with the composition $[Si_8O_{20}]$ found in agrellite have been found previously in fenaksite, $FeNaKSi_4O_{10}$ (Golovachev *et al.*, 1971), litidionite, $CuNaKSi_4O_{10}$ (Pozas *et al.*, 1975), and $CuNa_2Si_4O_{10}$ (Kawamura and Kawahara, 1977). In these three isostructural compounds, $[Si_8O_{20}]$ tubes are cross-linked by serrated chains of edge-sharing dimers of Fe- (or Cu-) square pyramids alternating with dimers of edge-sharing Na-square pyramids. The potassium atoms (likewise one set of sodium atoms in $CuNa_2Si_4O_{10}$) occur in cavities created by the boat-

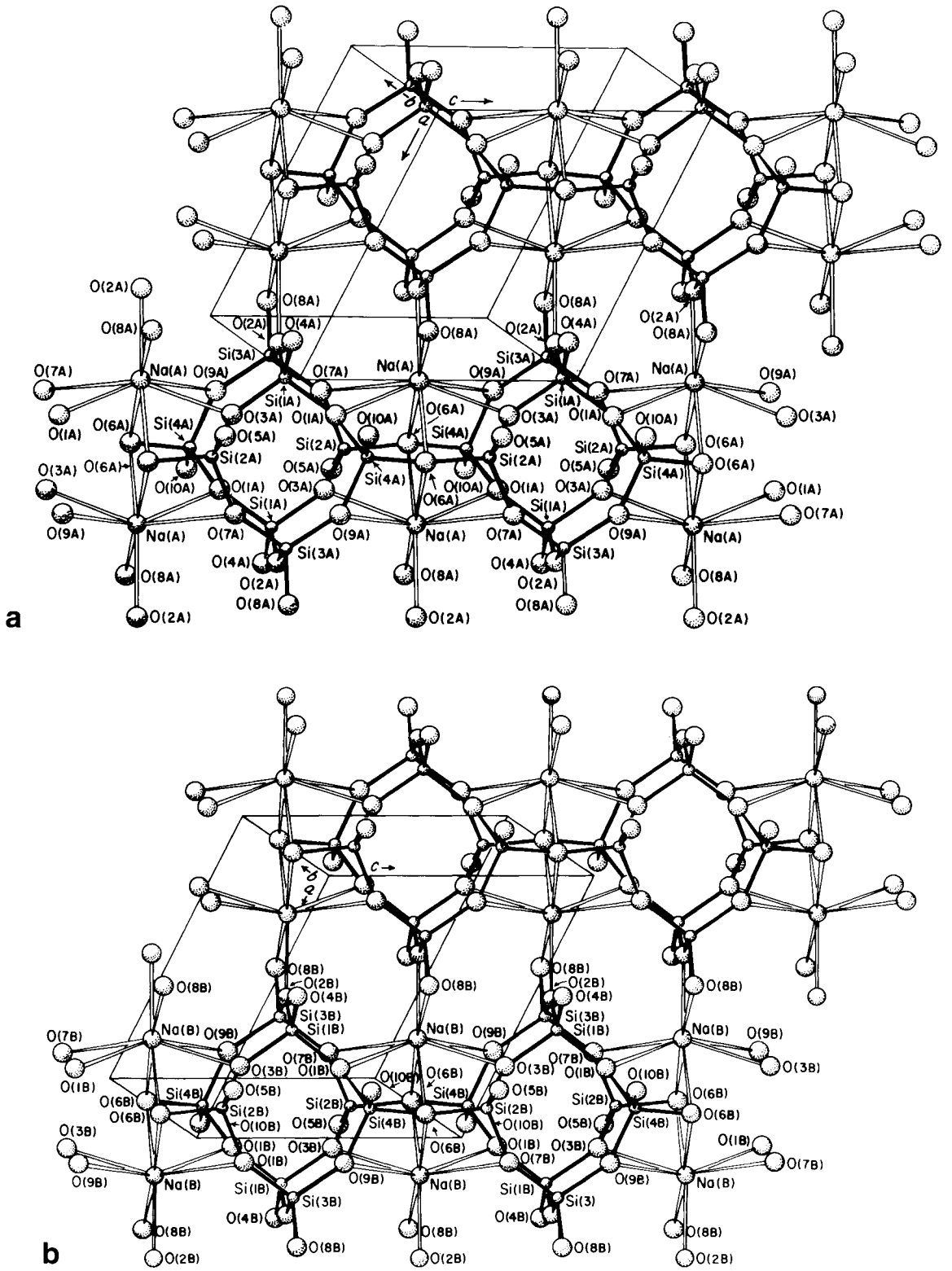

Fig. 3a,b. Agrellite: views of the two crystallographically distinct sodium silicate layers, *A* and *B*, parallel to the (010) plane.

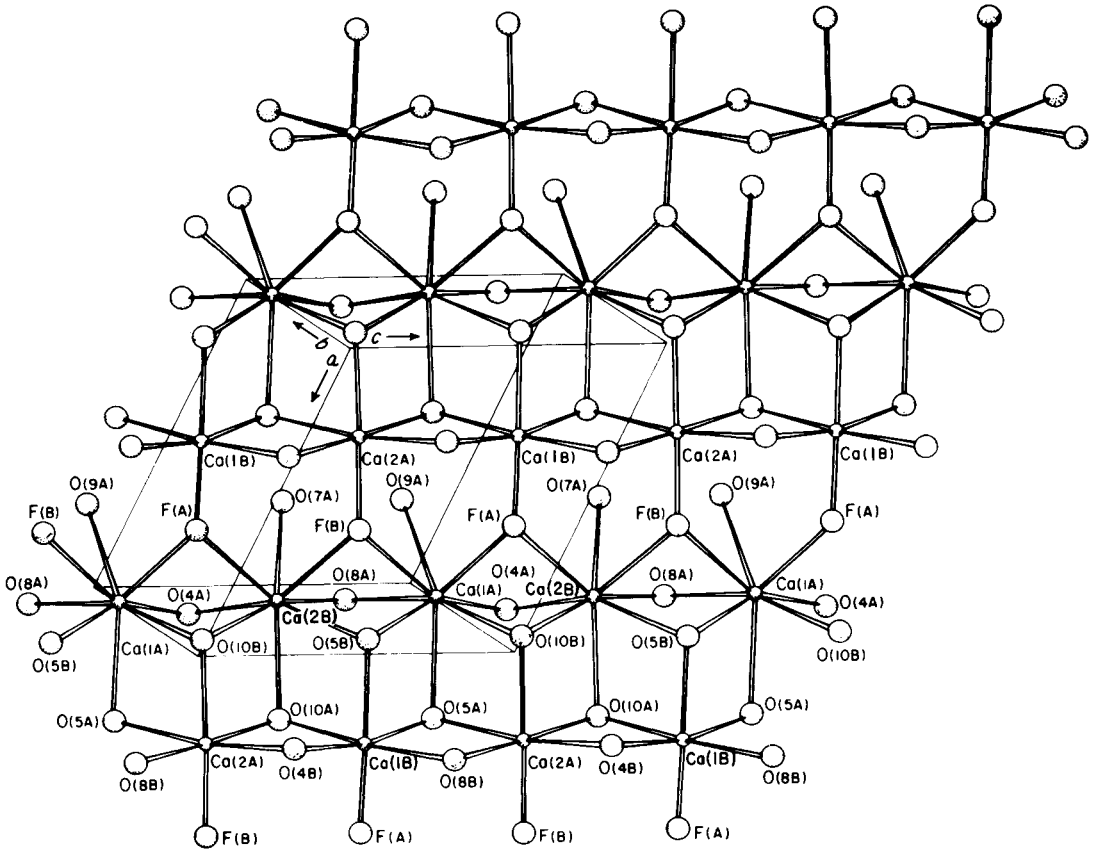

Fig. 4. Agrellite: a view of the calcium polyhedral layer parallel to the (010) plane.

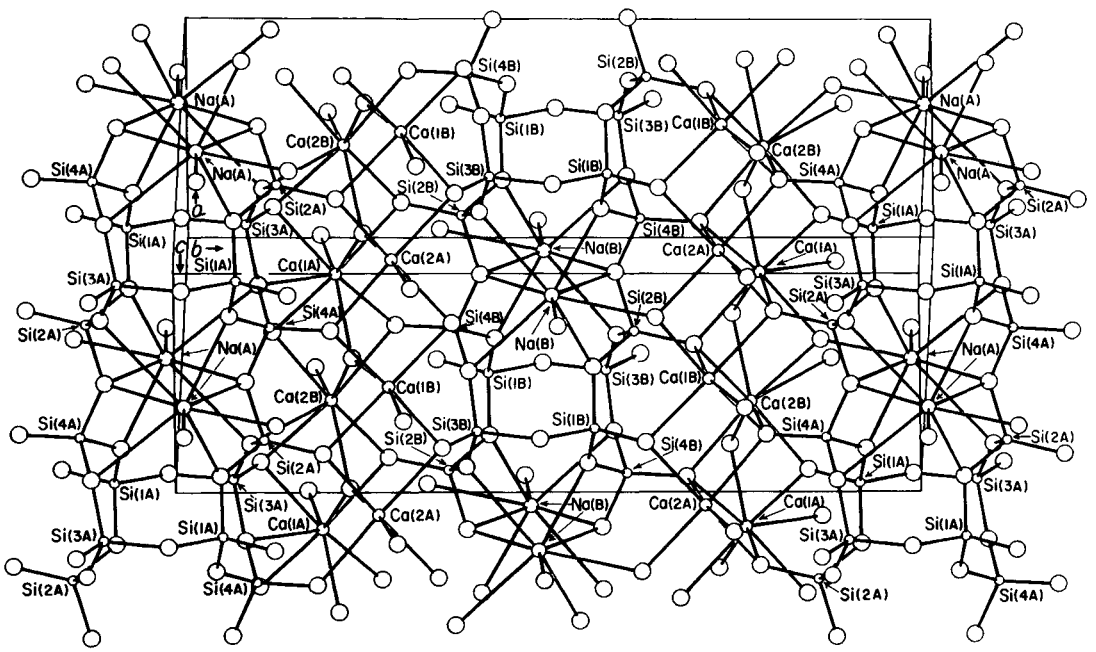

Fig. 5. Agrellite: a view along the *a* axis; note the stacking of the sodium silicate layers and the calcium polyhedral layers along the *b* axis.

shaped eight-membered tetrahedral rings, and are closely comparable to the Na-coordination found in agrellite. However, in agrellite there are two crystallographically-distinct double chains, whereas in these compounds there is only one. This distinction is most likely created by the different coordination requirements of calcium and fluorine atoms in agrellite, as opposed to the transition-metal ions in fenaksite and litidionite.

Liebau (1978) has termed the $[Si_8O_{20}]$ tube a "loop-branched *dreier* (three-tetrahedral-repeat) double chain." We would like to emphasize the tubular nature of these double chains and prefer to classify them in a group of structures composed of silicate tubes. The other members of this group are narsarsukite, $Na_2TiOSi_4O_{10}$ (Pyatenko and Pudovkina, 1959; Peacor and Buerger, 1962), canasite, $Ca_5Na_4K_2[Si_{12}O_{30}](OH,F)_4$ (Chiragov *et al.*, 1969), and miserite, $KCa_5(Si_2O_7)(Si_6O_{15})(OH,F)$ (Scott, 1976). The silicate tube in narsarsukite is defined by four-membered rings, whereas those in canasite and miserite are defined by two different types of eight-membered rings.

Acknowledgments

We are indebted to P. J. Dunn, Smithsonian Institution, for the donation of the agrellite crystal, and to Dr. Y. Ohashi, University of Pennsylvania, Philadelphia, and Dr. S. Guggenheim, University of Illinois at Chicago Circle, for critical reviews. This research has been supported in part through NSF grant EAR 76-13373 (Geochemistry).

References

Bond, W. L. (1951) Making small spheres. *Rev. Sci. Instr., 22,* 344–345.

Chiragov, M. I., Kh.S. Mamedov and N. V. Belov (1969) On the crystal structure of kanasite—$Ca_5Na_4K_2[Si_{12}O_{30}](OH,F)_4$. *Dokl. Akad. Nauk SSSR, 185,* 672–674 (in Russian).

Cromer, D. T. and D. Liberman (1970) Relativistic calculation of anomalous scattering factors for X-rays. *J. Chem. Phys., 53,* 1891–1898.

——— and J. B. Mann (1968) X-ray scattering factors computed from numerical Hartree-Fock wave functions. *Acta Crystallogr., A24,* 321–324.

Finger, L. W. (1969) Determination of cation distribution by least-squares refinement of X-ray data. *Carnegie Inst. Wash. Year Book, 67,* 216–217.

Fleet, S. G. and J. R. Cann (1967) Vlasovite: a second occurrence and a triclinic to a monoclinic inversion. *Mineral. Mag., 36,* 233–241.

Germain, G., P. Main and M. M. Woolfson (1971) The application of phase relationships to complex structures III. The optimum use of phase relationships. *Acta Crystallogr., A27,* 368–376.

Ghose, S. and C. Wan (1978a) A new type of silicate double chain in agrellite, $NaCa_2Si_4O_{10}F$. *Naturwissenschaften, 65,* 59.

——— (1978b) Zektzerite, $NaLiZrSi_6O_{15}$: a silicate with six-tetrahedral-repeat double chains. *Am. Mineral., 63,* 304–310.

Gittins, J., M. G. Bown and D. Sturman (1976) Agrellite, a rock-forming mineral in regionally metamorphosed agpaitic rocks. *Can. Mineral., 14,* 120–126.

Golovachev, V. P., Yu.N. Drozdov, E. A. Kuz'min and N. V. Belov (1971) The crystal structure of fenaksite. *Soviet Phys.—Dokl., 15,* 902–904.

Karle, J. and I. L. Karle (1966) The symbolic addition procedure for phase determination for centrosymmetric and non-centrosymmetric crystals. *Acta Crystallogr., 21,* 849–859.

Kawamura, K. and A. Kawahara (1977) The crystal structure of synthetic copper sodium silicate: $CuNa_2Si_4O_{10}$. *Acta Crystallogr., B33,* 1071–1075.

Liebau, F. (1978) Silicates with branched anions: a crystallochemically distinct class. *Am. Mineral., 63,* 918–923.

Peacor, D. R. and M. J. Buerger (1962) The determination and refinement of the structure of narsarsukite, $Na_2TiOSi_4O_{10}$. *Am. Mineral., 47,* 539–556.

Pozas, J. M. M., G. Rossi and V. Tazzoli (1975) Re-examination and crystal structure analysis of litidionite. *Am. Mineral., 60,* 471–474.

Pyatenko, Y. U. and Z. V. Pudovkina (1959) Concerning the crystal structure of narsarsukite. *Sov. Phys. Crystallogr., 12,* 885–886.

Scott, J. D. (1976) Crystal structure of miserite, a Zoltai type 5 structure. *Can. Mineral., 14,* 515–528.

Stewart, J. M., G. J. Kruger, H. L. Ammon, C. Dickinson and S. R. Hall (1972) The X-RAY SYSTEM—version of June, 1972. *Tech. Rep. TR-192,* Computer Science Center, University of Maryland, College Park, Maryland.

Tossell, J. A. and G. V. Gibbs (1977) Prediction of T–O–T angles from molecular orbital studies on corner sharing mineral fragments (abstr.). *Trans. Am. Geophys. Union, 58,* 522.

Wan, C. and S. Ghose (1978) Inesite, a hydrated calcium manganese silicate with five-tetrahedral-repeat double chains. *Am. Mineral., 63,* 563–571.

———, ——— and G. V. Gibbs (1977) Rosenhahnite, $Ca_3Si_3O_8(OH)_2$: crystal structure and the stereochemical configuration of the hydroxylated trisilicate group, $[Si_3O_8(OH)_2]$. *Am. Mineral., 62,* 503–512.

Voronkov, A. A. and Yu. A. Pyatenko (1961) Crystal structure of vlasovite (in Russian). *Kristallografiya, 6,* 937–943.

Manuscript received, January 12, 1978;
accepted for publication, December 19, 1978.